Structural determinants for selective recognition of peptide ligands for endothelin receptor subtypes ET$_A$ and ET$_B$

Jens Lättig,[a] Alexander Oksche,[b] Michael Beyermann,[a] Walter Rosenthal[a,b] and Gerd Krause[a]*

The molecular basis for recognition of peptide ligands endothelin-1, -2 and -3 in endothelin receptors is poorly understood. Especially the origin of ligand selectivity for ET$_A$ or ET$_B$ is not clearly resolved. We derived sequence-structure-function relationships of peptides and receptors from mutational data and homology modeling. Our major findings are the dissection of peptide ligands into four epitopes and the delineation of four complementary structural portions on receptor side explaining ligand recognition in both endothelin receptor subtypes. In addition, structural determinants for ligand selectivity could be described. As a result, we could improve the selectivity of BQ3020 about 10-fold by a single amino acid substitution, validating our hypothesis for ligand selectivity caused by different entrances to the receptors' transmembrane binding sites. A narrow tunnel shape in ET$_A$ is restrictive for a selected group of peptide ligands' *N*-termini, whereas a broad funnel-shaped entrance in ET$_B$ accepts a variety of different shapes and properties of ligands. Copyright © 2009 European Peptide Society and John Wiley & Sons, Ltd.

Supporting information may be found in the online version of this article

Introduction

The endothelin receptors belong to the rhodopsin-like family I (class A) of GPCRs with seven transmembrane-spanning helices and a short extracellular *N*-terminus. Out of the endothelin selective receptors [1–4], two receptor subtypes have been extensively studied: endothelin receptor subtype A (ET$_A$) and B (ET$_B$). Activation of these receptors is induced following binding of one of the endothelin isopeptides. The induced conformational changes of the receptor's transmembrane helices (TMHs) and intracellular loops lead subsequently to activation of G proteins and intracellular signaling processes. Both receptors are involved in a vast array of physiological processes, such as vasoconstriction/vasodilatation, bronchoconstriction, proliferation and hypertrophy of vascular smooth muscle cells, stimulation of astrocyte proliferation and modulation of neurotransmitter release [5–7].

ET$_A$ and ET$_B$ demonstrate different preferences in the recognition of the endothelin isopeptides endothelin-1 (ET-1), -2 (ET-2) and -3 (ET-3). ET$_A$ binds ET-1 and ET-2 with similar affinities, but ET-3 with 100-fold lower affinity [8]. In contrast, ET$_B$ recognizes all endothelin isoforms with similar affinities. A unique feature of ET$_B$, not shared by ET$_A$, is the quasi-irreversible binding of ET-1 based on the formation of a super-stable complex. As a consequence, this complex remains intact even in the presence of 2% SDS, an acidic environment, or the late endosomes and lysosomes [9,10].

Apart from ET-1, ET-2 and ET-3, sarafotoxins (Sfx6a, Sfx6b, Sfx6c, Sfx6d) being isolated from snake venom of *Atractaspis engaddensis* represent further naturally occurring agonists. All of the naturally occurring peptide ligands comprise 21 amino acids.

Structural information on two native peptide ligands is available at the Protein Data Base (PDB) [11]: an NMR structure of Sfx6b

(entry: 1srb) as well as NMR and X-ray data of ET-1 (entries: 1edn, 1edp, 1v6r) [12–15]. These data for ET-1 and Sfx6b show the ligand's *N*-terminal stretch (residues 1 to 7) linked to the central helix (residues 11 to 15) in an anti-parallel orientation. This is achieved by two disulfide bridges (Cys1–Cys15 and Cys3–Cys11) as well as linking residues 8 to 10. The *C*-terminus (residues 16 to 21) does not seem to have a fixed structure. X-ray crystallographic data of ET-1 (PDB entry: 1edn) report a helical structure for the ligand's *C*-terminal chain. As the crystal structure shows a parallel dimer along the *C*-terminal helices, the formation of this fold might be induced by the particular crystal measured. NMR-structures provide different conformations for the *C*-terminal chain. For ET-1 (PDB entry: 1v6r) an extended β-structure is reported, orienting hydrophobic residues Leu17 and Ile19 toward the central helix by forming a hydrophobic core around side chain Tyr13 [16]. In other NMR structures of ET-1 (PDB entry: 1edp) the *C*-terminus is not completely solved indicating some flexibility in this region (Figure 1). This is in agreement with Sfx6b (PDB entry: 1srb), where a flexible *C*-terminus is provided. Here, this might be because of
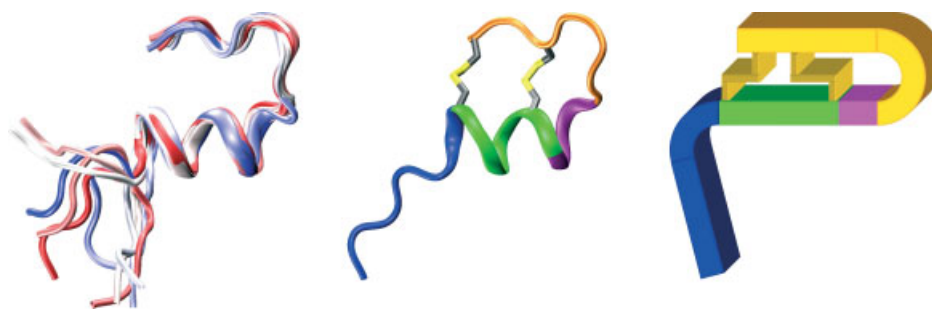
Figure 1. Overview on the structure of endothelin receptor selective peptide ligands. (a) Ensemble of NMR-structures of Sfx6b shows the restricted conformation of the *N*-terminal stretch and the flexible nature of the *C*-terminal residues in these peptides. (b) The *N*-terminus is restrained to the central helix via two disulfide bridges. (b, c) Dissected regions in peptide ligands are shown in color-coding (1^L – orange, 2^L – magenta, 3^L – green, 4^L – blue, see also Table 2), visualized in structure as well as in cartoon. Images of molecular structures created with VMD [93].

the exchange of Leu17Asn impeding the hydrophobic interaction around Tyr13 in ET-1.

Functional studies of interactions of peptide ligands with chimera receptors combining ET_A and ET_B revealed that the *C*-terminal peptide region binds to TMH4 through TMH6, whereas the *N*-terminus interacts with TMH1, TMH2, TMH3 and TMH7 [17]. Already short peptide constructs of residues from 16 to 21 are sufficient to inhibit the endothelin receptors [18–20]. The hydrophobic *C*-terminal residues Ile20 and Trp21 as well as the negatively charged residue Asp18 and the carboxyl group at the *C*-terminus are pivotal points in signal transduction [21,22]. Mutation or deletion of Trp21 abolishes the interactions with the receptors [23,24]. Similarly, amidation of the *C*-terminal carboxyl group (Trp21) represses ligand–receptor interactions [18]. In photo-labeling studies with endothelin receptor ligands TTA-386 and IRL1620 an orientation of the *C*-terminus of peptide ligands toward TMH5 was suggested [25].

The sequences of both receptor subtypes in their respective transmembrane regions reveal a high degree of similarity. Only few differences are found, which could contribute to ligand selectivity or other receptor subtype specific properties [26]. Substitutions at position 2.53 in TMH2 of ET_A (Tyr129Phe) and ET_B (His150Tyr) resulted in unaltered affinities for ET-1 and ET-2 [27,28]. In contrast, substitution Tyr129His in ET_A resulted in an increased affinity of ET-3 and Sfx6c, although still 10-fold to 10 000-fold less active than in ET_B [27–29]. Ligand binding sensitive mutations are reported for charged residues in TMH2 (Asp2.50, Asp2.57, Lys2.64) and TMH7 (Asp7.35) [30–34]. However, data on these mutants do not explain the high selectivity in the binding of peptide ligands in endothelin receptor subtypes. Thus, it has been suspected that the extracellular regions, such as the *N*-terminus and the three extracellular loops (ECLs) might contribute to ligand selectivity [35].

The molecular basis explaining ligand selectivity in ET_A and ET_B is poorly understood. In addition, the apparent binding affinities of peptide ligands such as ET-1 (0.01–0.06 nM) are remarkably an order of magnitude higher than those of small molecules such as Bosentan (4.7 nM) [34–37]. A detailed molecular description of peptide ligand recognition, binding and initial receptor activation has, therefore, a vital importance in understanding the molecular mechanisms in endothelin receptor action as well as in the design of new ligands with binding affinities comparable to ET-1.

Here, we assemble the existing experimental data on ligands and receptors and provide a systematic sequence–structure–function study of endothelin receptor peptide ligands and the counterpart sites in both endothelin receptor subtypes. We present molecular determinants for ligand selectivity in ET_A and ET_B as well as an improved ET_B-selective agonist. In addition, we describe molecular properties involved in the discrimination of agonists and antagonists at these receptors.

Material and Methods

Preparation of Peptides

Peptides were synthesized automatically (ABI 433A) by the solid-phase method using Fmoc [N-(9-fluorenyl)methoxycarbonyl] chemistry in a batch-wise mode as described previously for the synthesis of corticotropin releasing factor (CRF) analogs [38]. After final cleavage/deprotection using trifluoroacetic acid/H_2O (9/1), crude peptides were purified by preparative HPLC to give final products of 95% purity according to HPLC analysis. For cyclization (disulfide formation) linear peptide (1 mg/ml) was dissolved in sodium bicarbonate buffer at pH 8.5 (for acceleration 10–15 vol% dimethylsulfoxide may be added), and the mixture was stirred exposed to air for 2–3 days. After reduction of volume by lyophilization the product was purified by preparative HPLC and characterized by mass spectrometry, which gave the expected masses (Table 1).

^{125}I-Ligand Displacement Binding Experiments

Radioligand experiments were performed as described earlier [10]. In brief, membranes (0.1–0.5 μg) derived from HEK 293 cell clones either expressing the ET_A or the ET_B receptor were incubated in 200 μl of Tris/bacitracin/aprotinin/$MgCl_2$/EGTA buffer containing 50 pM ^{125}I-ligand (ET-1, BQ3020 derivative) without or with increasing concentrations of unlabeled ligand (1×10^{-13} to 1×10^{-4} M) for 3 h at 25 °C in a shaking water bath. The samples

Table 1. Analytical characterization of peptide ligands synthesized by mass spectrometry and analytical HPLC (uv 220 nm)

	$[M+H]^+$ calc.	$[M+H]^+$ found/purity [%]
ET-1	2401.04	2401.4/99.3
Cy3-ET-1	3142.3	3142.4/88.5
BQ3020	2005.9	2006.0/94.8
Cy3-BQ3020	2657.3	2657.5/91.6
BQ3020(Lys9Glu)	2006.9	2007.1/93.0

were then transferred to GF/C filters (Whatman) pretreated with 0.1% (w/v) polyethylenimine. The filters were washed twice with PBS using a Brandel cell harvester and transferred into 5-mL vials. Radioactivity was determined using a gamma counter. Data were analyzed with RadLig Software 4.0 (Cambridge, UK), and graphs were generated with Prism Software 2.01 (GraphPad, San Diego, CA, USA).

Generation of Receptor Models

The endothelin receptors of different species sorted by their subtypes ET_A and ET_B and in alignment with bovine rhodopsin were analyzed using SeqLab (Wisconsin Package Version 10.2, Accelrys Inc. San Diego, CA, USA).

Structure models of human endothelin receptor subtypes ET_A and ET_B are based on the structure of bovine rhodopsin entry 1hzx provided by the PDB [11,39]. The models were generated by side chain substitutions in the homologous transmembrane regions using SYBYL6.8 (Tripos Inc., St. Louis, MS, 63144, USA). Short loops were added by best fit and best homology using fragments of other proteins provided by LOOP SEARCH tool implemented in SYBYL6.8.

The models were generated with the following characteristics:

- The models comprising residues Cys69 to Cys386 in ET_A and Cys90 to Cys403 in ET_B
- The extracellular *N*-terminus is linked by a disulfide bridge to ECL3 (Cys69–Cys341 in ET_A and Cys90–Cys358 in ET_B)
- The conserved disulfide bridge in rhodopsin-like GPCRs between TMH3 and ECL2 has been kept (Cys158–Cys239 in ET_A and Cys174–Cys255 in ET_B)
- Owing to helix-forming motifs, helices TMH5, TMH6 and TMH7 were extracellularly extended
- Analogous to the intracellular extension observed in the crystal structure of bovine rhodopsin from PDB entry 1gzm [40], TMH5 and TMH6 were intracellularly extended
- Introduction of a proline kink in TMH2 based on a more homologous structure fragment of the sixth transmembrane helix of sensory rhodopsin II, from PDB entry 1jgj [41], altered the extracellular orientation of TMH2 to about 20° outward compared to the structure of bovine rhodopsin.

Resulting structures have been refined by optimization of side chain interactions and checked using Ramachandran plots. Endothelin receptor structure models have been optimized by steepest descent energy minimization using Amber4.1 force field with Amber95-Protein-ALL charges in SYBYL6.8 and a complete PROCHECK scan [42,43]. The particularities of rhodopsin-like GPCRs, such as the cysteine-bridge connecting TMH3 and ECL2, as well as the D(E)RY and NPxxY motifs, have been taken into consideration.

Ligand Docking

In the assembly of ligand–receptor complexes a docking protocol has been invented using an initial ligand docking step followed by a stability checking simulation in Amber7 [44] using *ff99* force field. Owing to the nature of endothelin ligand/endothelin receptor interaction, which is rather a protein/protein interaction, the available *ff02* force field that adds polarizable dipoles to atoms has not been applied. ET-1 (PDB entry: 1v6r) and Sf6b (PDB entry: 1srb) have been docked in ET_A and ET_B. In addition, IRL1038 has been docked in ET_B.

In the initial docking step (*in vacuo* simulation for 200 ps), the structure of receptor TMHs was kept by application of harmonic potential restraints on C_α carbons (5 kcal $\times$ mol^{-1}) whereas the loops were free to move. Dihedral restraints (5 kcal $\times$ mol^{-1}) were applied in peptide ligands to the central helix (residues Cys11 to Cys15) and side chains involved in disulfide linkage (Cys1–Cys15 and Cys3–Cys11). The ligand was positioned 10 Å above the receptor and pulled into the binding site using restraints (5 kcal $\times$ mol^{-1}) to experimentally known functional sensitive residues. These residues were considered as anchor points for interactions with the important ligand portions Asp18, Trp21 and the *C*-terminal carboxyl group. The procedure has been applied to each ligand–receptor complex five times to identify the most suitable docking poses. All structures have undergone a stability check in a 2-ns simulation without any restraints in a water–vacuum–water box [45]. The overall C_α RMSD remained below 1.8 nm, indicating stably formed ligand–receptor complexes.

The docking poses, showing best agreement with known experimental data from literature, have been selected for further observations. Docking restraints derived from literature data, resulting in these final docking poses, are tabulated (Table 2).

Results

Structural Differences Between ET_A and ET_B

The most striking sequence difference between ET_A and ET_B is an insertion of a mostly hydrophilic stretch of five amino acid residues (Asp149-His150-Asn151-Asp152-Phe153 in human) into the first ECL in ET_A. In addition, in ET_A the sequence of the *N*-terminus in close proximity to ECL1 displays a remarkably hydrophilic region as potential counterpart (His66-Asn67-Tyr68-Cys69-Pro70-Gln71-Gln72-Thr73-Lys74-Ile75-Thr76-Ser77) in contrast to the rather hydrophobic residues at the corresponding site in ET_B (Pro87-Pro88-Pro89-Cys90-Gln91-Gly92-Pro93-Ile94-Glu95-Ile96-Lys97-Glu98). As a consequence and in contrast to ET_B, additional interactions between the hydrophilic residues in the larger ECL1 and the hydrophilic region in the *N*-terminus can be built up in ET_A. Additional conformational differences may result from different locations of a proline residue in ECL2 in ET_A and ET_B, which is found either prior to (Pro228 in ET_A) or after (Pro259 in ET_B) the central cysteine (Cys239 in ET_A and Cys255 in ET_B), and two additionally inserted residues (Thr263-Ala264) in ET_B. According to our comparative molecular models, these sequence and structure differences in endothelin receptor subtypes provide strong support for differently shaped entrances to the transmembrane binding cleft: a narrow, tunnel-shaped entrance in ET_A and a broad, funnel-like entrance in ET_B (Figure 2).

Delineation of Peptide Ligands into Four Epitopes

In sequence–structure–function relationship studies, available functional data have been combined with ligand–receptor complex models and sequence alignment investigations of peptide ligands in relation to endothelin receptor specificity and effects on receptor stimulation. The following peptides, showing either common or selective preference for endothelin receptor subtypes, were examined: Endothelins ET-1, ET-2, ET-3, modified endothelins Ala^{1,15}ET-1, Ala^{3,11}ET-1, Ala^{1,3,11,15}ET-1, Ala^{11,15}ET-1(6–21), Ala^{11,15}ET-1(8–21), Ala^{11,15}ET-1(10–21), sarafotoxins Sfx6b, Sfx6c and peptide derivatives BQ3020, IRL1620 (all agonists) as well

Table 2. Data from site-directed mutagenesis experiments on endothelin receptors taken from literature and used as restraints in MD supported ligand docking. The effects on binding of these mutants are listed as increased ($+$), unchanged ($\pm$) or reduced ($-$)

Ballesteros' Numbering	Mutation Sites		Effects on Ligand Binding			
	in ET_A	in ET_B	ET-1	ET-2	ET-3	Restraint to Ligand Property
1.49	Gly97Ala [31]		$-$	$-$	$-$	
2.53	Tyr129Ala [27–28]		$\pm$	$\pm$	$+$	
	Tyr129Ser [27–28]		$\pm$	$\pm$	$+$	
	Tyr129Thr [28]		$\pm$	$-$	$+$	
	Tyr129Asn [27]		$\pm$	$\pm$	$+$	
	Tyr129Gln [27]		$\pm$	$\pm$	$+$	
	Tyr129His [27]		$\pm$	$\pm$	$+$	
	Tyr129Lys [27,28]		$\pm$	$\pm$	$+$	
	Tyr129Ile [28]		$\pm$	$-$	$+$	
	Tyr129Phe [27,28]		$\pm$	$\pm$	$+$	
	Tyr129Trp [28]		$\pm$	$-$	$\pm$	
		His150Ala [27]	$\pm$	$\pm$	$\pm$	
		His150Tyr [27]	$\pm$	$\pm$	$\pm$	
2.64	Lys140Ile [31–33]		$-$			*Asp18*
		Lys161Ile [32]			$-$	
3.26	Lys159Gln [31]		$-$			
3.32	Gln165Asp [31]		$-$			*C-term.*
3.33		Lys182Arg [79]	$\pm$	$-$	$-$	*C-term.*
		Lys182Ala [79]	$\pm$	$-$	$-$	
		Lys182Met [79]	$\pm$	$-$	$-$	
		Lys182Asp [79]	$\pm$	$-$	$-$	
		Lys182Glu [79]	$\pm$	$-$	$-$	
5.40	Trp257Ala [80]		$\pm$			
	Trp257Phe [80]		$\pm$			
		Trp275Ala [80]	$\pm$			
		Trp275Phe [80]	$\pm$			
5.41	Trp258Ala [80]		$\pm$			
		Trp276Ala [80]	$\pm$			
		Trp276Cys [80]	$\pm$			
5.46	Tyr263Phe [31]		$\pm$			
6.31		Arg319Trp [81,82]	$\pm$			
6.44	Phe315Leu [31]		$-$			*Trp21*
6.55	Arg326Gln [31]		$\pm$			
7.35	Arg351Asn [31]		$\pm$			

as the peptide antagonists IRL1038 and PD142893 (Table 3). We delineated four epitopes to the endothelin receptor peptide ligands: two selectivity providing regions 1^L (hydrophilic residues 1 to 7) and 2^L (charged residues 8 to 10); the affinity increasing 3^L region (hydrophobic residues 11 to 15); as well as the minimal ligand comprising 4^L region (residues 16 to 21). Moreover, the separation of the *N*-terminal part into two selectivity providing regions, 1^L and 2^L, additionally allows the explanation of agonism and antagonism.

Identification of Four Ligand-Sensitive Portions on Receptor Side

Our ligand–receptor complex models provided an assignment of distinct interaction sites for all four ligand epitopes at the receptor counterparts in ET_A and ET_B using complementary shapes and properties: a purely hydrophilic portion (A^R); a charged, edge-like portion (B^R); a hydrophobic portion (C^R); and a transmembrane binding cleft (D^R). The residues and locations comprising the

different ligand-sensitive portions on receptor side are tabulated in Tables 4 and 5.

Ligand–Receptor Interactions at the Binding Site

Interaction between ligands and receptors resulted in the following differences at four interfaces:

1^L–A^R: The receptors' A^R portions comprise the tunnel-shaped entrance in ET_A and the funnel-like entrance in ET_B (Figure 2(e), (f)). A^R in ET_A operates as selector for the 1^L epitope of peptide ligands. The narrow shape and the coated properties force the ligand into a defined orientation, where the small side chains of the 1^L epitope of ET-1 point between the *N*-terminal tail and ECL2/ECL3 in ET_A (Figure 3(a), (c)). In contrast, A^R in ET_B accepts peptide ligands with a large *N*-terminal variety of sequence and structure (Figure 3(b), (d)).

2^L–B^R: In molecular docking simulations the charged residues of 2^L epitopes of agonists ET-1 and Sfx6b caught B^R, a region of complementary charged residues in both receptor subtypes. In
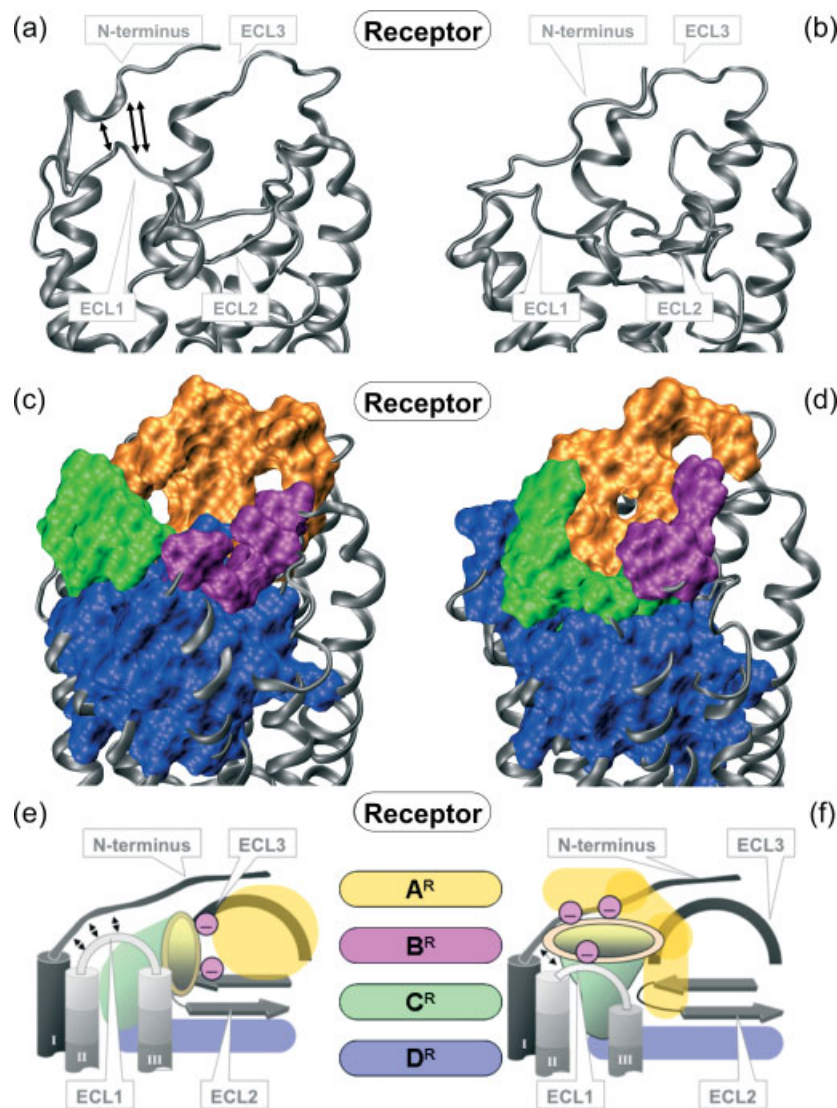
Figure 2. Schemes and models of ET_A/ET_B differences: Owing to sequence differences in ECL1, the structures of this loop vary between ET_A and ET_B. As a result, ET_A shows more interactions between ECL1 and the *N*-terminus (black arrows) than ET_B (a, b). These conformations result in different shapes of the extracellular entrances to the binding sites in both receptor subtypes. A narrow, restrictive tunnel-shaped entrance in ET_A (c) and a widened, funnel-like entrance in ET_B are formed (d) being responsible for differences in binding and selectivity of ligand peptides. The complete binding sites can be distinguished into four structural regions with different functions (e, f) shown in color-coding similar to the ligands (A^R – pale orange, B^R – pale magenta, C^R – pale green, D^R – pale blue). Images of molecular structures created with VMD [93].

contrast, the antagonist IRL1038 lacking the *N*-terminal portion including the charged 2^L sequence did not catch B^R and slid deeper into the transmembrane binding cleft. Resulting from the different A^R portions in ET_A and ET_B, the ligands bind in different orientations. This is supported by different localization of the charged residues of B^R in both receptor subtypes (Figures 2, 3, Table 4).

Our ligand–receptor complex models identified potential interaction partners within ECL2 in B^R in ET_A for the conserved 2^L epitope (Asp8-Lys9-Glu10) of ET_A-selective peptides. Comparison of the 2^L epitopes of ET_A- and ET_B-selective peptide ligands suggested position 9 with its large, positively charged side chain (Lys9) as the most suitable candidate in 2^L for our hypothesis of B^R determining ligand selectivity in ET_A/ET_B. Ligand binding experiments of ET_A- and ET_B-selective peptides, where the photo-label Cy3 has been attached to the amino group of Lys9, demonstrated the large

side chain being well accepted in both receptor subtypes (Table 6). The interaction site of Lys9 in our ligand–receptor complex models, which is more on the extracellular rim of the binding pocket, tolerates Cy3's volume because of a slightly solvent-exposed positioning of Lys9.

However, a shorter, negatively charged side chain in position 9 is found in the two most ET_B-selective agonists IRL1620 and Sfx6c (Table 3), suggesting a contribution to ET_B selectivity. To answer the question, if interactions between 2^L and B^R contribute to receptor selectivity, we intended to increase the selectivity of BQ3020 [46] for ET_B. BQ3020 is an ET_B-selective agonist but contains the 2^L epitope conserved in ET_A-selective ligands (Asp8-Lys9-Glu10) comprising a positive charge in position 9. Introducing the 2^L epitope of ET_B-selective IRL1620 (Asp8-Glu9-Glu10) containing a negative charge in position 9 into BQ3020 (BQ3020:Lys^{9}Glu) should result in improved

Table 3. Sequence alignment of investigated endothelins and endothelin-like ligands. The specificity for ET_B as well as the effects in modulation of endothelin receptors have been listed. Colored boxes at the bottom of the alignment highlight the delineated ligand epitopes 1^L, 2^L, 3^L and 4^L (F* = D-Diphenylalanine)

LIGAND NAME	LIGAND SEQUENCE	SPECIFICITY FOR ET_B	EFFECT ON RECEPTOR	REFERENCE
ET-1	C S C S S L M D K E C V Y F C H L D I I W-OH	~1-fold	Stimulation	(83)
ET-2	C S C S S W L D K E C V Y F C H L D I I W-OH	~1-fold	Stimulation	(84)
Sf6b	C S C K D M T D K E C L Y F C H Q D V I W-OH	~1-fold	Stimulation	(85)
ET-3	C T C F T Y K D K E C V Y Y C H L D I I W-OH	~100-fold	Stimulation	(84)
Sf6c	C T C N D M T D E E C L N F C H Q D V I W-OH	~1000-fold	Stimulation	(86)
Ala^{3,11}ET-1	C S A S S L M D K E A V Y F C H L D I I W-OH	~100-fold	Stimulation	(87)
Ala^{1,15}ET-1	A S C S S L M D K E C V Y F A H L D I I W-OH	~100-fold	Stimulation	(87)
Ala^{1,3,11,15} ET-1	A S A S S L M D K E A V Y F A H L D I I W-OH	~1000-fold	Stimulation	(88)
Ala^{11,15}ET-1(6-21)	L M D K E A V Y F A H L D I I W-OH	~1000-fold	Stimulation	(88)
BQ3020	Ac I M D K E A V Y F A H L D I I W-OH	~1000-fold	Stimulation	(89)
Ala^{11,15}ET-1(8-21)	D K E A V Y F A H L D I I W-OH	~1000-fold	Stimulation	(88)
Ala^{11,15}ET-1(10-21)	E A V Y F A H L D I I W-OH	~1000-fold	Stimulation	(88)
IRL-1620	Suc D E E A V Y F A H L D I I W-OH	~1000-fold	Stimulation	(90)
PD 142893	Ac F* L D I I W-OH	~1-fold	Inhibition	(91)
IRL-1038	A V Y F A H L D I I W-OH	~100-fold	Inhibition	(92)

Sequence position markers: 5, 10, 15, 20

Ligand epitope boxes: 1L, 2L, 3L, 4L

Table 4. Residues within the regions A^R, B^R and C^R forming the entrance to D^R, the transmembrane binding cleft, in ET_A and ET_B; the residues are based on our ligand–receptor complex models after stability checking MD simulations

	A^R		B^R		C^R	
	In ET_A	In ET_B	In ET_A	In ET_B	In ET_A	In ET_B
N-terminus	Cys69	Cys90			Glu95	Lys74
	Pro70	Gln91			Glu98	
	Gln71	Gly92				
	Gln72	Pro93				
		Ile94				
		Glu95				
		Lys97				
ECL1	Phe148	Glu165	Asn151	Glu165	Ala143	Trp167
	Asp149	Asp166		Asp166	Gly144	Pro168
		Trp167			Arg145	Phe169
					Trp146	Gly170
					Phe148	Ala171
					His150	
					Phe153	
ECL2	Gln235	Val260	Glu230	Asp246	Arg232	Tyr247
	Thr244	Gln261	Arg232	Lys248	Gly233	Lys248
	Ser245		Gln235	Gln261	Thr244	Tyr251
	Lys246					Leu252
						Phe259
						Val260
ECL3	Met336	Arg357				
	Asp337	Cys358				

Table 5. Interaction partners for the *C*-terminal epitope 4^L in agonists (e.g. endothelins, sarafotoxins) in both endothelin receptor subtypes; residues have been identified after stability checking MD simulations

Peptide Residue	Interaction Partner at		Ballesteros–Weinstein Numbering [91]	Subtype-Specific Difference in ET_A/ET_B
	ET_A	ET_B		
His16	Asn83	Asn104	**1.35**	–
	Tyr352	Tyr369	**7.36**	–
Leu17	Gly154	Gly170	**3.21**	–
	Val155	Ala171	**3.22**	X
	Leu157	Met173	**3.24**	X
	Cys158	Cys174	**3.25**	–
Asp18	Lys80	Lys101	**1.32**	–
	Lys140	Lys161	**2.64**	–
Ile19	Phe161	Val177	**3.28**	X
	Pro162	Pro178	**3.29**	–
Ile20	Leu322	Leu339	**6.51**	–
	Ile355	Ile372	**7.39**	–
	Ala358	Ala375	**7.42**	–
Trp21 (indole moiety)	Phe264	Phe282	**5.47**	–
	Trp319	Trp336	**6.48**	–
Trp21 (carboxyl group)	Lys166	Lys182	**3.33**	

Table 6. Binding data of peptide ligands ET-1 and BQ3020 as well as their Lys9-Cy3 labeled derivatives in both endothelin receptor subtypes

	K_i for Binding in	
	ET_A	ET_B
	Mean $\pm$ SD ($n = 3$)	Mean $\pm$ SD ($n = 3$)
ET-1	0.057 ± 0.021 nM	0.035 ± 0.006 nM
Cy3-ET-1	0.045 ± 0.027 nM	0.036 ± 0.011 nM
BQ3020	49 ± 17 nM	0.155 ± 0.161 nM
Cy3-BQ3020	36 ± 26 nM	0.79 ± 0.44 nM

ET_B selectivity. Indeed, ligand binding experiments using BQ3020:Lys^{9}Glu showed decreased affinity for ET_A, whereas that for ET_B was not affected (Table 7). As a consequence, BQ3020:Lys^{9}Glu has a 10-fold increased selectivity for ET_B compared to BQ3020 (Table 7) and confirms the interactions between 2^L and B^R as decisive and important selectivity filter. $3^L – C^R$: The hydrophobic C^R portion, which is located at the junctions of ECL1 with TMH2 and TMH3 as well as in ECL2 (Figures 2(e), (f), 3(a), (b)), interacts with hydrophobic residues 12 to 14 of 3^L (in ET-1: Val12-Tyr13-Phe14). These interactions, especially π-stacking contacts of the involved aromatic residues, seem to provide energy benefits for high affinity binding.

$4^L – D^R$: Our ligand docking studies provide evidence for the above-suggested ability of the *C*-terminal ligand residues to adopt varying spatial orientations. The *C*-terminal flexibility of endothelin receptor peptide ligands allows to bind the ligand 4^L epitope within the transmembrane binding cleft D^R, despite the different orientations of the other ligand portions (1^L, 2^L, 3^L) enforced by the different entrances A^R in ET_A and ET_B (Figures 1, 3).

D^R, which is located between TMHs 2, 3, 5, 6 and 7, is large and contains overlapping antagonistic and agonistic binding sites. The potential $4^L – D^R$ interaction partners are tabulated (Table 5). The difference between agonistic and antagonistic ligand actions is determined by the presence and absence of the charged 2^L epitope (see $2^L – B^R$ above). In agonists, 4^L remained restrained in a position within D^R closer to the extracellular surface, where its *C*-terminal residues Ile20 and Trp21 enforced reorientations of nearby receptor side chains

(e.g. Trp6.48, Figure 4(a)). In contrast, 4^L of antagonists slid deep into the internal membrane region of D^R, adopting similar orientation in endothelin receptors as 11-*cis*-retinal in the inactive structure of bovine rhodopsin (Figure 4(b), (c)). The induced side chain orientations (especially Phe5.47, Trp6.48), being different to those of agonists, most likely constrain the inactive state of the receptor.

To facilitate the comparison of different GPCRs, we used the Ballesteros–Weinstein nomenclature [47] for residues in the transmembrane helix bundle.

Discussion

Since the first citation of ET-1 in 1988, several investigations on the endothelins and sarafotoxins as well as their derivatives were made [48]. Whereas *N*-terminal modifications in these peptides generally affected the binding to ET_A more, modifications in the *C*-terminus reduced or abolished interactions with both receptor subtypes. Out of this, Menziani *et al.* concluded that the *C*-termini of peptide ligands are 'highly important in

Table 7. Binding data of BQ3020 and its derivative BQ3020:Lys^{9}Glu in ET$_A$ and ET$_B$ demonstrates the increase of ET$_B$ selectivity by a negative charge in position 9 of peptide agonists

	K_i for Binding in		ET$_B$-Specificity
	ET$_A$	ET$_B$	
	Mean $\pm$ SD ($n = 3$)	Mean $\pm$ SD ($n = 3$)	
BQ3020	49 ± 17 nM	0.155 ± 0.161 nM	$\sim$100-fold
BQ3020(Lys9Glu)	412 ± 192 nM	0.191 ± 0.050 nM	$\sim$1000-fold
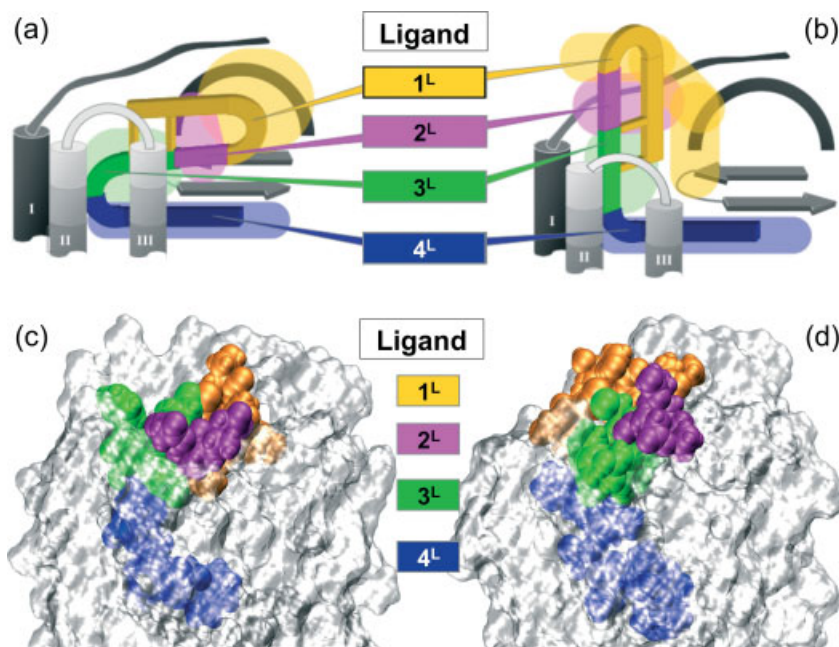
Figure 3. Ligand binding in endothelin receptor subtypes. Ligands and receptors have been dissected each in four different regions, which are color-coded (see Figure 1, 2 and Table 3). The interactions appear in both receptors between $1^L–A^R$, $2^L–B^R$, $3^L–C^R$ and $4^L–D^R$. The large differences between receptor subtypes are the shapes of the entrances and the properties in the receptors' A^R regions. In ET$_A$ (a) the tunnel-like entrance results in well-defined interactions of 1^L epitope and A^R region and a very restrictive binding mode. In ET$_B$ (b) the broad and funnel-like entrance allows several interactions at A^R, which tolerates peptides with more different *N*-termini by nonselective ligand interactions. Color-coded structure models of ET-1 in ET$_A$ and Sfx6b in ET$_B$, being the result of MD simulations, are shown in (c) and (d), respectively. Images of molecular structures created with VMD [93].

receptor recognition and signal transduction' by interaction with the transmembrane binding cleft, whereas the *N*-termini 'might bind to residues located at the entrance of the binding cleft conferring high affinity and selectivity to the peptide' [35]. Following the classical principle of receptor–hormone interactions via 'address' and 'message' epitopes suggested earlier [49], we dissect here the sequence of native peptide ligands into four epitopes based on sequence–structure–function relationships (Table 3, Figure 1). In addition, the receptor binding sites in ET$_A$ and ET$_B$ can be delineated into four structural portions, which are complementary in shape and properties to the ligand regions (Figure 2). Our data further provide strong evidence of structural differences in the extracellular entrance portions in ET$_A$ and ET$_B$ (Figure 2(a)–(f), sequence alignment provided in Supporting Information, Figure S1) resulting in different participation of extracellular receptor portions in ligand recognition (Figure 3(a), (b)). Similar evidence has been shown recently by using Endothelin-derived photoprobes [50].

Owing to the high sequence similarity within the serpentine domains of both receptor subtypes as well as the recently shown irrelevance of ET$_B$'s *N*-terminus in ligand binding [51],

we propose a more conserved mechanism in ligand recognition by a cooperative participation of transmembrane helices and juxtaposed extracellular loops. Therewith, our models of ET$_A$ and ET$_B$ are different to the models between ET-1 and ET$_A$ described earlier [52,53].

$1^L–A^R$ Interaction Is the Main Selectivity Filter

The anti-parallel *N*-terminal stretch 1^L in native peptide ligands is the most variable region in endothelin receptor agonists. 1^L plays a pivotal role in selective binding to ET$_A$ and ET$_B$ as several lines of evidence support. Comparison of peptide ligand sequences to their endothelin receptor selectivity (Table 3) shows that differences of the three *N*-terminal residues to the ET-1 sequence lead to decreased affinity for ET$_A$ and result in increased selectivity for ET$_B$. Peptides lacking the *N*-terminal stretch 1^L, such as the mainly α-helical IRL1620 [54], are ET$_B$-selective ligands. They bind to ET$_B$ with similar affinity as native peptide ligands, whereas their affinity for ET$_A$ is 100-fold to 10 000-fold lower than the affinity of ET-1. We hypothesize that any ET-1-like peptide sequence without an anti-parallel orientation of the *N*-terminal stretch 1^L to the central helix portion is generally structured as
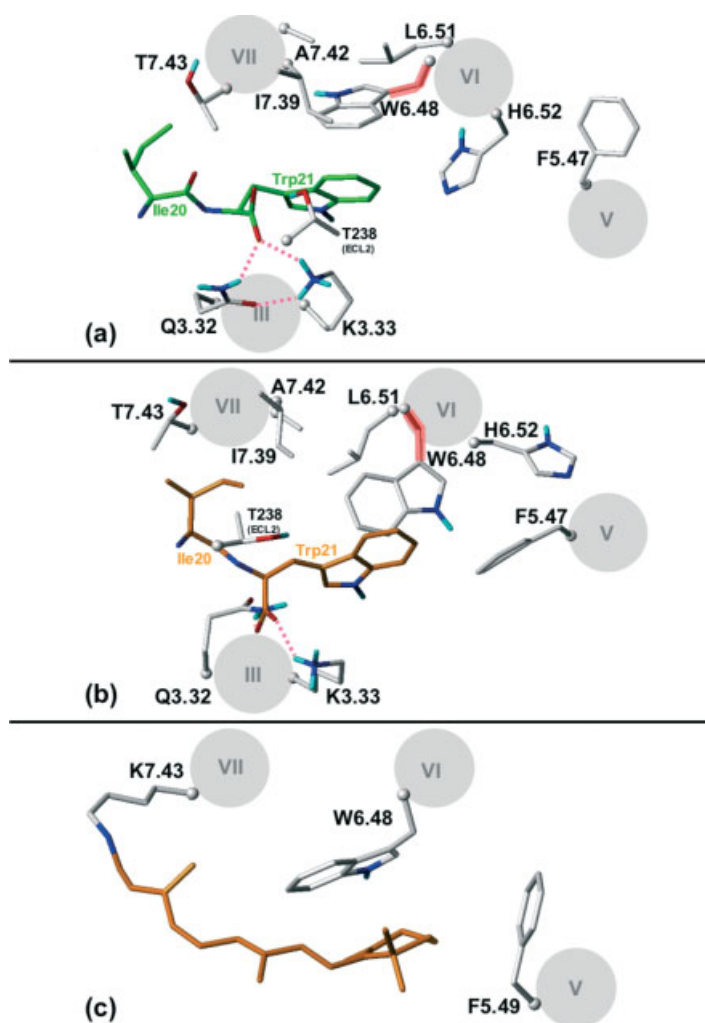
Figure 4. Comparison of interactions in 4^L-D^R as derived from MD simulations. The last two *C*-terminal residues Ile20 and Trp21, which are known to be essential for receptor binding, are shown. (a) Agonistic peptides: residues Ile20 and Trp21 (green) are restrained – by the 2^L-B^R interaction (not shown) – in a location between TMH3 (III), 6 (VI) and 7 (VII) closer to the extracellular surface. As a consequence, Trp21 causes changes in side chain orientation of Trp6.48 and nearby side chains (Leu6.51, His6.52), which subsequently leads to a dispersion of helix TMH6 (VI) compared to the inactive conformation. The change in side chain orientation of Trp6.48, which is highlighted in red in (a) and (b), is based on a rotamer toggle. (b) Antagonistic peptides: Owing to the missing 2^L-B^R interaction, antagonists slide differently into the binding cleft orienting Ile20 and Trp21 in a position between TMH3–6 (III, IV, V, VI) deep inside the internal membrane region. As a result, Trp21 preserves the orientation of Trp6.48 side chain in the inactive receptor state. (c) X-ray structure of bovine rhodopsin (dark state, inactive receptor): The relative spatial location and orientation of the β-ionone ring of 11-*cis*-retinal (orange) and Trp6.48 of rhodopsin match the identical location and mutual orientation of the antagonist's Trp21 indole-ring toward Trp6.48 in endothelin receptors supporting the antagonist model in (b). Images of molecular structures created with MOE [94].

straight α-helix. This structure does not find optimal interactions in the narrow, tunnel-like A^R region in ET_A resulting in reduced affinity in this receptor subtype. On the contrary, the broad, funnel-like A^R in ET_B easily tolerates such modifications. As a result, such peptides are ET_B-selective ligands [55–57].

2^L-B^R Interaction Provides Additional Features for Selectivity

The ligand's 2^L epitope is contained in endothelin receptor agonists and connects the *N*-terminal stretch 1^L with the central helix 3^L. Peptides stimulating ET_A share a conserved Asp8-Lys9-Glu10 motif (Table 3). But ET_B-selective peptides often contain an acidic residue in position 9 (Table 3). Literature data from site-directed mutagenesis experiments at this position in ET-1 reported no significant affinity changes in ET_A and ET_B for the substitution to leucine [8]. However, the substitution of ET-1's Lys9 to alanine and glutamate has been described as relevant for

receptor subtype selectivity [58]. Owing to this, the existence or absence of a long (Lys9) or bulky (Leu9) side chain might, besides charge interactions, be another selectivity providing feature. This further explains why attaching the Cy3 chromophor to the side chain of Lys9 does not result in significant changes in receptor affinity, despite removing the residue's positive charge.

2^L-B^R Interaction Separates the Agonists from the Antagonists

The 2^L epitope is a common ligand portion to all endothelin receptor agonists, but not receptor antagonists PD142893 and IRL1038 (Table 3). Modifications of Asp8 or Glu10 in ET-1 to amino acids with comparable length but altered electrostatic properties result in loss of function (Asp8Asn, Asp8Lys, Glu10Gln, Glu10Lys) [8,58,59]. However, replacements of these residues to alanine decrease peptide activity but not affinity and suggest that the

observed loss of function is not based on abolished receptor interaction [23]. These alanine scans further demonstrated Asp8 as most important residue within 2^L, determining agonist properties. Ligands with Asp8Ala bind with wt-affinity but rather act as antagonists (stimulatory effect 1/100 of wt-peptide).

3^L–C^R Interaction Generates Certain Energy Gain Necessary for High Affinity Binding

The naturally occurring endothelin receptor agonists and their peptide derivates share the hydrophobic 3^L epitope. Variations in the amino acid sequence of this region are very small and only of conservative nature. The replacement of Cys11 and Cys15 by alanine dramatically reduces the binding in ET_A but not in ET_B, which is most probably based on the formation of 1^L (see 1^L–A^R). It is notable that all investigated peptide ligands centrally display a helical structure [12–15,46,55–57,59]. Thus, the residues 12, 13 and 14 (in ET-1: Val12–Tyr13–Phe14) are optimally oriented for interactions with the mainly aromatic, hydrophobic residues in C^R at the receptor's extracellular junction of TMH2 and TMH3. As a consequence, modifications in this ligand region, altering the hydrophobic environment, lead to complete loss of ligand binding, as found for alanine replacements of Val12, Tyr13 or Phe14 [8,23]. We, therefore, conclude that the interactions between 3^L and C^R lead to important energy benefits in binding. We further hypothesize that these energy benefits may be responsible for high affinity in peptide ligand–endothelin receptors interactions.

4^L–D^R Interaction Modulates Receptor Activation and Inhibition

The 4^L epitope of peptide ligands is highly conserved in agonists and antagonists (Table 3). Owing to the size of the peptide ligands, the 4^L epitope interacts in our structure models within the 'classic' GPCR binding site of small ligands consisting of TMH3–6 [60–65] as well as in the recently described binding site between TMH2, -3 and -7 [66–68]. This orientation is in agreement with data on the interaction of peptide ligands in endothelin receptors [17]. The negative charge of *C*-terminal carboxyl group anchors the ligand on Lys3.33 in both receptor subtypes, which is consistent with experimental data where removal of the *C*-terminal negative charge by amidation resulted in abolished ligand interaction [18].

According to our models, the molecular differences of peptide ligand-induced receptor inhibition and activation can be explained by the absence and existence of negative charges in the 2^L epitope of peptide ligands as a counterpart of the B^R region in receptors (see above).

Our computational models on receptor inhibition by assembling ET_B with the antagonist IRL1038 show the *C*-terminal residues Ile20 and Trp21, which have been described as crucially relevant in receptor activation [23], deep inside the membrane region in D^R. The residues match comparable interaction partners in ET_B as 11-*cis*-retinal in rhodopsin (Figure 4(b), (c)). In addition, Trp21 shows comparable location and orientation regarding Trp6.48 as the β-ionone ring of 11-*cis*-retinal in the inactive dark state of rhodopsin. Owing to this, we suggest the interactions of Ile20 and Trp21 in antagonists to be restraining the inactive state in endothelin receptors, which explains the antagonistic nature of the *C*-terminal hexapeptide [35].

On the contrary, our investigations on agonist–receptor complexes revealed Ile20 and Trp21 to be oriented closer to the extracellular surface and shifted to TMH3, -6 and -7 within D^R. This caused a change in side chain orientation of Trp6.48 (Figure 4(a)), very likely driving TMH6 apart. The reorientation provoked by Trp21 is based on π-stacking contacts as experimental data of Trp21 mutation to nonaromatic residues abolished the interaction [23] but mutations to aromatic amino acids were tolerated [58].

Observed changes in side chain conformations at TMH6 are in agreement with a 'rotamer toggle switch', which has been recently reported in other GPCRs for the conserved Trp6.48 during activation [69,70]. This similarity indicates the orientation of Ile20 and Trp21 within D^R closer to the extracellular surface to be necessary in endothelin receptor activation. It further suggests the interaction of 2^L and B^R as a discriminator for agonists to be true.

Evaluation of Our Models Regarding Existing Structural Data

Reported low RMSD values between backbones of the transmembrane helices of the rhodopsin structure and the recently solved X-ray structures of β1- and β2-adrenergic receptor (PDB entry codes: 2R4R, 2RH1) as well as A2A adenosine receptor (PDB entry code: 3EML) support the reliability of our $ET_{A/B}$-TMH models, which are based on rhodopsin structure [71–75].

The major structural difference in X-ray crystallographic data concerns ECL2. However, out of the current structure templates only rhodopsin provides an ECL2 structure with high sequence similarity in sequence length and side chain properties to the ECL2 sequences of ET_A and ET_B. In addition, specific cysteines in ECL2 (two additional cysteines in β1-and β2-adrenergic receptor and four in A2A adenosine receptor) form additional cysteine bridges stabilizing a helical fold in ECL2 of these receptors. Neither in ET_A nor ET_B such cysteine residues are included. As a consequence, we kept a rhodopsin-like β-hairpin structure and location of ECL2 also in our $ET_{A/B}$ models. Additionally, the rhodopsin-like ECL2 conformation is consistent with results of diverse studies at other GPCRs [76–78]. Moreover, the different tunnel- and funnel-like entrance shapes for $ET_{A/B}$ occur irrespective of the used templates, which are based on the interaction of two hydrophilic sequence epitopes in ET_A that are not present in ET_B. The conserved nature of these differences of sequences suggests structural and functional importance. Although modeling of reliable loop structures in proteins is very difficult, we think that the significant differences between the extracellular entrances are modeled according to the currently available closest structural template.

Conclusion

Taken together, systematic sequence–structure–function analysis on peptide ligands and endothelin receptor subtypes ET_A and ET_B provides complementary molecular patterns resulting in better understanding of recognition mechanisms in peptide binding and receptor subtype selectivity. Moreover and apart from the activation mechanism, we suggest here a novel mode of action for peptide antagonists on the molecular level.

Supporting information

Supporting information may be found in the online version of this article.

References

1 Adachi M, Yang YY, Furuichi Y, Miyamoto C. Cloning and characterization of cDNA encoding human A-type endothelin receptor. *Biochem. Biophys. Res. Commun.* 1991; **180**(3): 1265–1272.

2 Karne S, Jayawickreme CK, Lerner MR. Cloning and characterization of an endothelin-3 specific receptor (ETC receptor) from Xenopus laevis dermal melanophores. *J. Biol. Chem.* 1993; **268**(25): 19126–19133.

3 Nakamuta M, Takayanagi R, Sakai Y, Sakamoto S, Hagiwara H, Mizuno T, Saito Y, Hirose S, Yamamoto M, Nawata H. Cloning and sequence analysis of a cDNA encoding human non-selective type of endothelin receptor. *Biochem. Biophys. Res. Commun.* 1991; **177**(1): 34–39.

4 Nambi P, Pullen M, Kincaid J, Nuthulaganti P, Aiyar N, Brooks DP, Gellai M, Kumar C. Identification and characterization of a novel endothelin receptor that binds both ET_A- and ET_B-selective ligands. *Mol. Pharmacol.* 1997; **52**(4): 582–589.

5 Wong SK. G protein selectivity is regulated by multiple intracellular regions of GPCRs. *Neurosignals.* 2003; **12**(1): 1–12. Review.

6 Miyauchi T, Masaki T. Pathophysiology of endothelin in the cardiovascular system. *Annu. Rev. Physiol.* 1999; **61**: 391–415. Review.

7 Davenport AP. International Union of Pharmacology. XXIX. Update on endothelin receptor nomenclature. *Pharmacol. Rev.* 2002; **54**(2): 219–226. Review.

8 Nakajima K, Kubo S, Kumagaye S, Nishio H, Tsunemi M, Inui T, Kuroda H, Chino N, Watanabe TX, Kimura T, Sakakibara S. Structure–activity relationship of endothelin: importance of charged groups. *Biochem. Biophys. Res. Commun.* 1989; **163**(1): 424–429.

9 Takasuka T, Sakurai T, Goto K, Furuichi Y, Watanabe T. Human endothelin receptor ET_B. Amino acid sequence requirements for super stable complex formation with its ligand. *J. Biol. Chem.* 1994; **269**(10): 7509–7513.

10 Oksche A, Boese G, Horstmeyer A, Furkert J, Beyermann M, Bienert M, Rosenthal W. Late endosomal/lysosomal targeting and lack of recycling of the ligand-occupied endothelin B receptor. *Mol. Pharmacol.* 2000; **57**(6): 1104–1113.

11 Berman HM, Westbrook J, Feng Z, Gilliland G, Bhat TN, Weissig H, Shindyalov IN, Bourne PE. The Protein Data Bank. *Nucleic Acids Res.* 2000; **28**(1): 235–242.

12 Atkins AR, Martin RC, Smith R. 1H NMR studies of sarafotoxin SRTb, a nonselective endothelin receptor agonist, and IRL 1620, an ET_B receptor-specific agonist. *Biochemistry.* 1995; **34**(6): 2026–2033.

13 Andersen NH, Chen CP, Marschner TM, Krystek SR, Bassolino DA, Jr. Conformational isomerism of endothelin in acidic aqueous media: a quantitative NOESY analysis. *Biochemistry.* 1992; **31**(5): 1280–1295.

14 Takashima H, Mimura N, Ohkubo T, Yoshida T, Tamaoki H, Kobayashi Y. Distributed computing and NMR constraint-based high-resolution structure determination: applied for bioactive Peptide endothelin-1 to determine *C*-terminal folding. *J. Am. Chem. Soc.* 2004; **126**(14): 4504–4505.

15 Janes Janes RW, Peapus DH, Wallace BA. The crystal structure of human endothelin. *Nat. Struct. Biol.* 1994; **1**(5): 311–319.

16 Takashima H, Tamaoki H, Teno N, Nishi Y, Uchiyama S, Fukui K, Kobayashi Y. Hydrophobic core around tyrosine for human endothelin-1 investigated by photochemically induced dynamic nuclear polarization nuclear magnetic resonance and matrix-assisted laser desorption ionization time-of-flight mass spectrometry. *Biochemistry.* 2004; **43**(44): 13932–13936.

17 Sakamoto A, Yanagisawa M, Sawamura T, Enoki T, Ohtani T, Sakurai T, Nakao K, Toyo-oka T, Masaki T. Distinct subdomains of human endothelin receptors determine their selectivity to endothelinA-selective antagonist and endothelinB-selective agonists. *J. Biol. Chem.* 1993; **268**(12): 8547–8553.

18 Rovero P, Galoppini C, Laricchia-Robbio L, Mazzoni MR, Revoltella RP. Structure–activity analysis of *C*-terminal endothelin analogues. *J. Cardiovasc. Pharmacol.* 1998; **31**(Suppl 1): S251–S254.

19 Macchia M, Barontini S, Ceccarelli F, Galoppini C, Giusti L, Hamdan M, Lucacchini A, Martinelli A, Menchini E, Mazzoni MR, Revoltella RP, Romagnoli F, Rovero P. Toward the rational development of peptidomimetic analogs of the *C*-terminal endothelin hexapeptide: development of a theoretical model. *Farmaco.* 1998; **53**(8–9): 545–556.

20 van der Walle CF, Barlow DJ. Investigations of structural requirements for endothelin antagonism. *Curr. Med. Chem.* 1998; **5**(4): 321–335. Review.

21 Forget MA, Lebel N, Sirois P, Boulanger Y, Battistini B, Fournier A. Structure–activity studies of the C-terminal segment of structurally reduced analogues of ET-1. *J. Cardiovasc. Pharmacol.* 1995; **26**(Suppl 3): S107–S110.

22 Forget MA, Lebel N, Sirois P, Boulanger Y, Fournier A. Biological and molecular analyses of structurally reduced analogues of endothelin-1. *Mol. Pharmacol.* 1996; **49**(6): 1071–1079.

23 Tam JP, Liu W, Zhang JW, Galantino M, Bertolero F, Cristiani C, Vaghi F, de Castiglione R. Alanine scan of endothelin: importance of aromatic residues. *Peptides.* 1994; **15**(4): 703–708.

24 Nakajima K, Kumagaye S, Nishio H, Kuroda H, Watanabe TX, Kobayashi Y, Tamaoki H, Kimura T, Sakakibara S. Synthesis of endothelin-1 analogues, endothelin-3, and sarafotoxin S6b: structure–activity relationships. *J. Cardiovasc. Pharmacol.* 1989; **13**(Suppl 5): S8–12; discussion S18.

25 Boivin S, Tessier S, Aubin J, Lampron P, Detheux M, Fournier A. Identification of a binding domain of the endothelin-B receptor using a selective IRL-1620-derived photoprobe. *Biochemistry.* 2004; **43**(36): 11516–11525.

26 Köchl R, Alken M, Rutz C, Krause G, Oksche A, Rosenthal W, Schülein R. The signal peptide of the G protein-coupled human endothelin B receptor is necessary for translocation of the *N*-terminal tail across the endoplasmic reticulum membrane. *J. Biol. Chem.* 2002; **277**(18): 16131–16138.

27 Lee JA, Elliott JD, Sutiphong JA, Friesen WJ, Ohlstein EH, Stadel JM, Gleason JG, Peishoff CE. Tyr-129 is important to the peptide ligand affinity and selectivity of human endothelin type A receptor. *Proc. Natl. Acad. Sci. USA.* 1994; **91**(15): 7164–7168.

28 Webb ML, Patel PS, Rose PM, Liu EC, Stein PD, Barrish J, Lach DA, Stouch T, Fisher SM, Hadjilambris O, Lee H, Skwish S, Dickinson KE, Krystek SR, Jr. Mutational analysis of the endothelin type A receptor (ET_A): interactions and model of selective ET_A antagonist BMS-182874 with putative ET_A receptor binding cavity. *Biochemistry.* 1996; **35**(8): 2548–2556.

29 Krystek SR, Patel PS, Rose PM, Fisher SM, Kienzle BK, Lach DA, Liu EC, Lynch JS, Novotny J, Webb ML, Jr. Mutation of peptide binding site in transmembrane region of a G protein-coupled receptor accounts for endothelin receptor subtype selectivity. *J. Biol. Chem.* 1994; **269**(17): 12383–12386.

30 Rose PM, Krystek SR, Patel PS, Liu EC, Lynch JS, Lach DA, Fisher SM, Webb ML, Jr. Aspartate mutation distinguishes ET_A but not ET_B receptor subtype-selective ligand binding while abolishing phospholipase C activation in both receptors. *FEBS Lett.* 1995; **361**(2–3): 243–249.

31 Breu V, Hashido K, Broger C, Miyamoto C, Furuichi Y, Hayes A, Kalina B, Löffler BM, Ramuz H, Clozel M. Separable binding sites for the natural agonist endothelin-1 and the non-peptide antagonist bosentan on human endothelin-A receptors. *Eur. J. Biochem.* 1995; **231**(1): 266–270.

32 Adachi M, Furuichi Y, Miyamoto C. Identification of specific regions of the human endothelin-B receptor required for high affinity binding with endothelin-3. *Biochim. Biophys. Acta.* 1994; **1223**(2): 202–208.

33 Adachi M, Furuichi Y, Miyamoto C. Identification of a ligand-binding site of the human endothelin-A receptor and specific regions required for ligand selectivity. *Eur. J. Biochem.* 1994; **220**(1): 37–43; Erratum in: *Eur. J. Biochem.* 1994; **221**(3): 1133.

34 Vichi P, Whelchel A, Posada J. Transmembrane helix 7 of the endothelin B receptor regulates downstream signaling. *J. Biol. Chem.* 1999; **274**(15): 10331–10338.

35 Menziani M, Cocchi M, Fanelli F, De Benedetti PG, Sanz F, Giraldo J, Manaut F. Theoretical QSAR analysis on three dimensional models of the complexes between peptide and non-peptide antagonists with the ET_A and ET_B receptors. In *QSAR and Molecular Modelling: Concepts, Computational Tools and Biological Applications*, Prous Science Publishers: Barcelona, Spain, 1995; 519–525.

36 Clozel M, Breu V, Gray GA, Kalina B, Löffler BM, Burri K, Cassal JM, Hirth G, Müller M, Neidhart W, Ramuz H. Pharmacological characterization of bosentan, a new potent orally active nonpeptide endothelin receptor antagonist. *J. Pharmacol. Exp. Ther.* 1994; **270**(1): 228–235.

489

37 Gregan B, Jürgensen J, Papsdorf G, Furkert J, Schaefer M, Beyermann M, Rosenthal W, Oksche A. Ligand-dependent differences in the internalization of endothelin A and endothelin B receptor heterodimers. *J. Biol. Chem.* 2004; **279**(26): 27679–27687.

38 Coin I, Beyermann M, Bienert M. Solid phase peptide synthesis: from standard procedure to the synthesis of difficult sequences. *Nature Protocols* 2007; **2**: 3247–3256.

39 Teller DC, Okada T, Behnke CA, Palczewski K, Stenkamp RE. Advances in determination of a high-resolution three-dimensional structure of rhodopsin, a model of G-protein-coupled receptors (GPCRs). *Biochemistry.* 2001; **40**(26): 7761–7772. Review.

40 Li J, Edwards PC, Burghammer M, Villa C, Schertler GF. Structure of bovine rhodopsin in a trigonal crystal form. *J. Mol. Biol.* 2004; **343**(5): 1409–1438.

41 Luecke H, Schobert B, Lanyi JK, Spudich EN, Spudich JL. Crystal structure of sensory rhodopsin II at 2.4 angstroms: insights into color tuning and transducer interaction. *Science.* 2001; **293**(5534): 1499–1503.

42 Cornell WD, Cieplak P, Bayly CI, Gould IR, Merz KM, Ferguson DM, Spellmeyer DC, Fox T, Caldwell JW, Kollman PA. A 2nd generation force-field for the simulation of proteins, nucleic-acids, and organic molecules. *J. Am. Chem. Soc.* 1995; **117**: 5179–5197.

43 Laskowski RA, MacArthur MW, Moss DS, Thornton JM. PROCHECK – a program to check the stereochemical quality of protein structures. *J. Appl. Cryst.* 1993; **26**: 283–291.

44 Case DA, Pearlman DA, Caldwell JW, Cheatham TE, III Wang J, Ross WS, Simmerling CL, Darden TA, Merz KM, Stanton RV, Cheng AL, Vincent JJ, Crowley M, Tsui V, Gohlke H, Radmer RJ, Duan Y, Pitera J, Massova I, Seibel GL, Singh UC, Weiner PK, Kollman PA. AMBER 7, 2002, University of California, San Francisco.

45 ter Laak AM, Kühne R. Bacteriorhodopsin in a periodic boundary water–vacuum–water box as an example towards stable molecular dynamics simulations of G-protein coupled receptors. *Receptors Channels.* 1999; **6**(4): 295–308.

46 Hewage CM, Jiang L, Parkinson JA, Ramage R, Sadler IH. Design of ET(B) receptor agonists: NMR spectroscopic and conformational studies of ET7-21[Leu7, Aib11, Cys(Acm)15]. *Protein Eng.* 2002; **15**(3): 161–167.

47 Ballesteros JA, Weinstein H. Integrated methods for the construction of three-dimensional models and computational probing of structure–function relationships in G-protein coupled receptors. *Methods Neurosci.* 1995; **25**: 366–428.

48 Itoh Y, Yanagisawa M, Ohkubo S, Kimura C, Kosaka T, Inoue A, Ishida N, Mitsui Y, Onda H, Fujino M, Masaki T. Cloning and sequence analysis of cDNA encoding the precursor of a human endothelium-derived vasoconstrictor peptide, endothelin: identity of human and porcine endothelin. *FEBS Lett.* 1988; **231**(2): 440–444.

49 Hechter O, Calek A, Jr. Principles of hormone action: the problem of molecular linguistics. *Acta. Endocrinol. Suppl. (Copenh).* 1974; **191**: 39–66.

50 Aubin J, Létourneau M, Francoeur E, Burgeon E, Fournier A. Identification of ET_A and ET_B binding domains using ET-derived photoprobes. *Biochimie.* 2008; **90**(6): 918–929.

51 Grantcharova E, Furkert J, Reusch HP, Krell HW, Papsdorf G, Beyermann M, Schulein R, Rosenthal W, Oksche A. The extracellular N terminus of the endothelin B (ET_B) receptor is cleaved by a metalloprotease in an agonist-dependent process. *J. Biol. Chem.* 2002; **277**(46): 43933–43941.

52 Bhatnagar S, Rao GS. Molecular modeling of the complex of endothelin-1 (ET-1) with the endothelin type A (ET(A)) receptor and the rational design of a peptide antagonist. *J. Biomol. Struct. Dyn.* 2000; **17**(6): 957–964.

53 Orry AJ, Wallace BA. Modeling and docking the endothelin G-protein-coupled receptor. *Biophys. J.* 2000; **79**(6): 3083–3094.

54 Katahira R, Umemura I, Takai M, Oda K, Okada T, Nosaka AY. Structural studies on endothelin receptor subtype B specific agonist IRL 1620 [suc-[Glu9, Ala11,15]ET(8–21)] and its analogs with dipalmitoyl phosphatidylcholine vesicles by NMR spectroscopy. *J. Pept. Res.* 1998; **51**(2): 155–164.

55 Hewage CM, Jiang L, Parkinson JA, Ramage R, Sadler IH. Development of ET(B) selective agonists: solution structure of a linear endothelin-1 analogue, ET-1 [Cys(Acm)(1,15), Ala3, Leu7, dAsp8, Aib11]. *J. Biomol. Struct. Dyn.* 1998; **16**(2): 425–435.

56 Hewage CM, Jiang L, Parkinson JA, Ramage R, Sadler IH. Solution conformation of an ET(B) selective agonist, ET-1[Cys(Acm)1,15,Ala3,Leu7,Aib11], in CD3OH/H2O by 1H NMR and molecular modelling. *FEBS Lett.* 1998; **425**(2): 234–238.

57 Hewage CM, Jiang L, Parkinson JA, Ramage R, Sadler IH. Solution structure of a novel ET_B receptor selective agonist ET1-21 [Cys(Acm)1,15, Aib3,11, Leu7] by nuclear magnetic resonance spectroscopy and molecular modelling. *J. Pept. Res.* 1999; **53**(3): 223–233.

58 Ergul A, Tackett RL, Puett D. Identification of receptor binding and activation sites in endothelin-1 by use of site-directed mutagenesis. *Circ. Res.* 1995; **77**(6): 1087–1094.

59 Watanabe TX, Itahara Y, Nakajima K, Kumagaye S, Kimura T, Sakakibara S. The biological activity of endothelin-1 analogues in three different assay systems. *J. Cardiovasc. Pharmacol.* 1991; **17**(Suppl 7): S5–S9.

60 Bonini JA, Jones KA, Adham N, Forray C, Artymyshyn R, Durkin MM, Smith KE, Tamm JA, Boteju LW, Lakhlani PP, Raddatz R, Yao WJ, Ogozalek KL, Boyle N, Kouranova EV, Quan Y, Vaysse PJ, Wetzel JM, Branchek TA, Gerald C, Borowsky B. Identification and characterization of two G protein-coupled receptors for neuropeptide FF. *J. Biol. Chem.* 2000; **275**(50): 39324–39331.

61 Ji TH, Grossmann M, Ji I. G protein-coupled receptors. I. Diversity of receptor–ligand interactions. *J. Biol. Chem.* 1998; **273**(28): 17299–17302. Review.

62 Kristiansen K. Molecular mechanisms of ligand binding, signaling, and regulation within the superfamily of G-protein-coupled receptors: molecular modeling and mutagenesis approaches to receptor structure and function. *Pharmacol. Ther.* 2004; **103**(1): 21–80. Review.

63 Shi L, Javitch JA. A role for information collection, management, and integration in structure–function studies of G-protein coupled receptors. *Curr. Pharm. Des.* 2006; **12**(14): 1771–1783. Review.

64 Stenkamp RE, Teller DC, Palczewski K. Crystal structure of rhodopsin: a G-protein-coupled receptor. *Chembiochem.* 2002; **3**(10): 963–967. Review.

65 Strader CD, Fong TM, Tota MR, Underwood D, Dixon RA. Structure and function of G protein-coupled receptors. *Annu. Rev. Biochem.* 1994; **63**: 101–132. Review.

66 He W, Miao FJ, Lin DC, Schwandner RT, Wang Z, Gao J, Chen JL, Tian H, Ling L. Citric acid cycle intermediates as ligands for orphan G-protein-coupled receptors. *Nature.* 2004; **429**(6988): 188–193.

67 Stitham J, Stojanovic A, Merenick BL, O'Hara KA, Hwa J. The unique ligand-binding pocket for the human prostacyclin receptor. Site-directed mutagenesis and molecular modeling. *J. Biol. Chem.* 2003; **278**(6): 4250–4257.

68 Tunaru S, Lättig J, Kero J, Krause G, Offermanns S. Characterization of determinants of ligand binding to the nicotinic acid receptor GPR109A (HM74A/PUMA-G). *Mol. Pharmacol.* 2005; **68**(5): 1271–1280.

69 McAllister SD, Hurst DP, Barnett-Norris J, Lynch D, Reggio PH, Abood ME. Structural mimicry in class A G protein-coupled receptor rotamer toggle switches: the importance of the F3.36(201)/W6.48(357) interaction in cannabinoid CB1 receptor activation. *J. Biol. Chem.* 2004; **279**(46): 48024–48037.

70 Swaminath G, Deupi X, Lee TW, Zhu W, Thian FS, Kobilka TS, Kobilka B. Probing the beta2 adrenoceptor binding site with catechol reveals differences in binding and activation by agonists and partial agonists. *J. Biol. Chem.* 2005; **280**(23): 22165–22171.

71 Cherezov V, Rosenbaum DM, Hanson MA, Rasmussen SG, Thian FS, Kobilka TS, Choi HJ, Kuhn P, Weis WI, Kobilka BK, Stevens RC. High-resolution crystal structure of an engineered human beta2-adrenergic G protein-coupled receptor. *Science.* 2007; **318**(5854): 1258–1265.

72 Rasmussen SG, Choi HJ, Rosenbaum DM, Kobilka TS, Thian FS, Edwards PC, Burghammer M, Ratnala VR, Sanishvili R, Fischetti RF, Schertler GF, Weis WI, Kobilka BK. Crystal structure of the human beta2 adrenergic G-protein-coupled receptor. *Nature.* 2007; **450**(7168): 383–387.

73 Rosenbaum DM, Cherezov V, Hanson MA, Rasmussen SG, Thian FS, Kobilka TS, Choi HJ, Yao XJ, Weis WI, Stevens RC, Kobilka BK. GPCR engineering yields high-resolution structural insights into beta2-adrenergic receptor function. *Science.* 2007; **318**(5854): 1266–1273.

74 Warne T, Serrano-Vega MJ, Baker JG, Moukhametzianov R, Edwards PC, Henderson R, Leslie AG, Tate CG, Schertler GF. Structure of

a beta1-adrenergic G-protein-coupled receptor. *Nature.* 2008; **454**(7203): 486–491.

75 Jaakola VP, Griffith MT, Hanson MA, Cherezov V, Chien EY, Lane JR, Ijzerman AP, Stevens RC. The 2.6 Angstrom crystal structure of a human A2A adenosine receptor bound to an antagonist. *Science* 2008; **322**(5905): 1211–1217.

76 Dragic T, Trkola A, Lin SW, Nagashima KA, Kajumo F, Zhao L, Olson WC, Wu L, Mackay CR, Allaway GP, Sakmar TP, Moore JP, Maddon PJ. Amino-terminal substitutions in the CCR5 coreceptor impair gp120 binding and human immunodeficiency virus type 1 entry. *J. Virol.* 1998; **72**(1): 279–285.

77 Aarons EJ, Beddows S, Willingham T, Wu L, Koup RA. Adaptation to blockade of human immunodeficiency virus type 1 entry imposed by the anti-CCR5 monoclonal antibody 2D7. *Virology.* 2001; **287**(2): 382–390.

78 Kleinau G, Claus M, Jaeschke H, Mueller S, Neumann S, Paschke R, Krause G. Contacts between extracellular loop two and transmembrane helix six determine basal activity of the thyroid-stimulating hormone receptor. *J. Biol. Chem.* 2007; **282**(1): 518–525.

79 Lee JA, Brinkmann JA, Longton ED, Peishoff CE, Lago MA, Leber JD, Cousins RD, Gao A, Stadel JM, Kumar CS, Ohlstein EH, Gleason JG, Elliott JD. Lysine 182 of endothelin B receptor modulates agonist selectivity and antagonist affinity: evidence for the overlap of peptide and non-peptide ligand binding sites. *Biochemistry.* 1994; **33**(48): 14543–14549.

80 Imamura F, Arimoto I, Fujiyoshi Y, Doi T. W276 mutation in the endothelin receptor subtype B impairs Gq coupling but not Gi or Go coupling. *Biochemistry.* 2000; **39**(4): 686–692.

81 Fuchs S, Amiel J, Claudel S, Lyonnet S, Corvol P, Pinet F. Functional characterization of three mutations of the endothelin B receptor gene in patients with Hirschsprung's disease: evidence for selective loss of Gi coupling. *Mol. Med.* 2001; **7**(2): 115–124.

82 Abe Y, Sakurai T, Yamada T, Nakamura T, Yanagisawa M, Goto K. Functional analysis of five endothelin-B receptor mutations found in human Hirschsprung disease patients. *Biochem. Biophys. Res. Commun.* 2000; **275**(2): 524–531.

83 Yanagisawa M, Kurihara H, Kimura S, Tomobe Y, Kobayashi M, Mitsui Y, Yazaki Y, Goto K, Masaki T. A novel potent vasoconstrictor peptide produced by vascular endothelial cells. *Nature.* 1988; **332**(6163): 411–415.

84 Yanagisawa M, Masaki T. Molecular biology and biochemistry of the endothelins. *Trends Pharmacol. Sci.* 1989; **10**(9): 374–378. Review.

85 Aimoto S, Hojoh H, Takasaki C. Studies on the disulfide bridges of sarafotoxins. Chemical synthesis of sarafotoxin S6B and its homologue with different disulfide bridges. *Biochem. Int.* 1990; **21**(6): 1051–1057.

86 Williams DL, Jones KL, Pettibone DJ, Lis EV, Clineschmidt BV, Jr. Sarafotoxin S6c: an agonist which distinguishes between endothelin receptor subtypes. *Biochem. Biophys. Res. Commun.* 1991; **175**(2): 556–561.

87 Randall MD, Douglas SA, Hiley CR. Vascular activities of endothelin-1 and some alanyl substituted analogues in resistance beds of the rat. *Br. J. Pharmacol.* 1989; **98**(2): 685–699.

88 Saeki T, Ihara M, Fukuroda T, Yamagiwa M, Yano M. [Ala1,3,11,15]endothelin-1 analogs with ET_B agonistic activity. *Biochem. Biophys. Res. Commun.* 1991; **179**(1): 286–292.

89 Peter MG, Davenport AP. Characterization of the endothelin receptor selective agonist, BQ3020 and antagonists BQ123, FR139317, BQ788, 50235, Ro462005 and bosentan in the heart. *Br. J. Pharmacol.* 1996; **117**(3): 455–462.

90 Takai M, Umemura I, Yamasaki K, Watakabe T, Fujitani Y, Oda K, Urade Y, Inui T, Yamamura T, Okada T. A potent and specific agonist, Suc-[Glu9,Ala11,15]-endothelin-1(8–21), IRL 1620, for the ET_B receptor. *Biochem. Biophys. Res. Commun.* 1992; **184**(2): 953–959.

91 Doherty AM, Cody WL, DePue PL, He JX, Waite LA, Leonard DM, Leitz NL, Dudley DT, Rapundalo ST, Hingorani GP, Haleen SJ, Ladouceur DM, Hill KE, Flynn MA, Reynolds EE. Structure–activity relationships of C-terminal endothelin hexapeptide antagonists. *J. Med. Chem.* 1993; **36**(18): 2585–2594.

92 Urade Y, Fujitani Y, Oda K, Watakabe T, Umemura I, Takai M, Okada T, Sakata K, Karaki H. An endothelin B receptor-selective antagonist: IRL 1038, [Cys11-Cys15]-endothelin-1(11–21). *FEBS Lett.* 1992; **311**(1): 12–16.

93 Humphrey W, Dalke A, Schulten K. "VMD–Visual Molecular Dynamics". *J. Molec. Graphics.* 1996; **14**: 33–38. vol. pp.

94 *Molecular Operating Environment (MOE), Version 2008.10*, Chemical Computing Group, Inc.: Montreal, Quebec, Canada 2008; http://www.chemcomp.com.